Journal of Cosmology and Astroparticle Physics
An IOP and SISSA journal

Received: *December 5, 2024*
Revised: *January 8, 2025*
Accepted: *February 24, 2025*
Published: *April 16, 2025*

BAO vs. SN evidence for evolving dark energy

Alessio Notari[a,b] **Michele Redi**[c,d] **and Andrea Tesi**[c,d]

[a] *Departament de Física Quàntica i Astrofisíca & Institut de Ciencies del Cosmos (ICCUB), Universitat de Barcelona, Martí i Franquès 1, 08028 Barcelona, Spain*
[b] *Galileo Galilei Institute for theoretical physics, Centro Nazionale INFN di Studi Avanzati, Largo Enrico Fermi 2, I-50125, Firenze, Italy*
[c] *INFN Sezione di Firenze, Via G. Sansone 1, I-50019 Sesto Fiorentino, Italy*
[d] *Department of Physics and Astronomy, University of Florence, Via G. Sansone 1, I-50019 Sesto Fiorentino, Italy*

E-mail: notari@fqa.ub.edu, michele.redi@fi.infn.it, andrea.tesi@fi.infn.it

Abstract: We critically review the evidence for time-varying dark energy from recent Baryon Acoustic Oscillations (BAO) and Supernova (SN) observations. First, we show that such evidence is present at the 3σ level, even without the new BAO data from the dark energy Spectroscopic Instrument (DESI), by instead using BAO data from the dark energy Survey (DES), combined with the DES5Y supernovae and Planck CMB data. Next, we examine the role of the DES5Y supernova dataset, showing that the preference for time-varying dark energy is driven by the low redshift supernovae common to both the DES5Y and Pantheon+ compilations. We find that combining Pantheon+ and DES5Y supernovae by removing the common supernovae leads to two different results, depending on whether they are removed from the DES5Y or the Pantheon+ catalog, leading to stronger or weaker exclusion of ΛCDM, at the (3.8σ) and (2.5σ) level, respectively. These common supernovae have smaller error bars in DES5Y compared to Pantheon+, and, as recently pointed out, there is an offset in magnitude in DES5Y between supernovae at $(z > 0.1)$, where almost all the measurements taken during the full five years of DES are, and the low-redshift ones $(z < 0.1)$, where all the historical set of nearby supernovae lies. We show that marginalizing over such an offset in DES5Y would lead to significantly weaker evidence for evolving dark energy.

Keywords: dark energy experiments, supernova type Ia - standard candles, baryon acoustic oscillations, cosmological parameters from LSS

ArXiv ePrint: 2411.11685

https://doi.org/10.1088/1475-7516/2025/04/048

JCAP04(2025)048

Contents

JCAP04(2025)048

1 Introduction and status

Learning that dark energy (DE) changes in time would be the greatest scientific result since the discovery of the accelerated expansion of the Universe itself, and it would have implications for fundamental physics both at the phenomenological and theoretical level. For this reason testing if DE is just a cosmological constant (Λ) or if it possibly has a time evolution is a very active experimental and observational field as it will establish the range of validity of the ΛCDM model.

Since the Universe has just "recently" entered its accelerated expansion phase, the search for time dependencies of dark energy has to rely on observables that are sensitive to the scale factor, $a(t)$, of the Friedmann-Robertson-Walker (FRW) metric background, at relatively recent cosmic times t, or redshifts z, on the possible largest scales.

It turns out that a very useful quantity is the so-called transverse diameter distance $D_M(z)$, defined — for a spatially flat universe — as the integral of the inverse Hubble parameter

$$D_M(z) \equiv \int_0^z \frac{dz'}{H(z')}\,, \tag{1.1}$$

where we used $c = 1$ units. The Hubble scale $H(z)$ is determined by the total energy density of the Universe at each redshift, through the Friedmann equation, and therefore D_M is sensitive to a possible time evolution of DE, which at late time dominates the energy density budget, $\Omega_{\rm DE} \approx 70\%$. Luckily, such a quantity D_M is directly related to two of the main observables available in the late universe: the luminosity flux from supernovae (SN), and the angle related to the so-called Baryon Acoustic Oscillations (BAO). It comes with no surprise that these two have received great attention in recent times.

In particular, the recent determination of the BAO at different redshift bins by the dark energy Spectroscopic Instrument (DESI) [1] has sparked an intense debate on the nature of DE (see for example [2, 3]). The claim can be quickly summarized by saying that the collaboration found significant evidence for an evolving DE component.

This conclusion has been reached thanks to two main steps. First, the collaboration has tested the hypothesis that DE is parametrized as a fluid with a time-dependent equation of state w,

$$w(z) = w_0 + w_a \frac{z}{1+z}\,, \tag{1.2}$$

following the Chevallier-Polarski-Linder parametrization [4, 5]. Second, the final result has been reached — crucially — by combining the DESI BAO measurements with Planck CMB data in combination with a SN dataset. This leads to w_0w_aCDM favoured compared to ΛCDM at the $2.5\sigma, 3.5\sigma$ and 3.9σ level depending on the SN dataset considered, i.e. Pantheon+ [6, 7], DES5Y [8] or Union3 [9] SN datasets respectively.

Both steps can be reconsidered in a more complete analysis. However, despite the fact that the best-fit values for the new parameters w_0 and w_a correspond to a fluid with a pathological equation of state at early times ($w < -1$), we will not reconsider here the theoretical model, and we will use the same parametrization of (1.2). Let us notice, however, that consistent models (which can be realized with a simple and healthy quintessence scalar field) in agreement with the claim of [1] have already been presented in the literature [10–18]. We refer to those papers for all the theoretical considerations, and we will leave the discussion aside in this work.

Instead, the primary focus of our work is to carefully re-examine the claims in [1] from the point of view of data analysis, taking inspiration by the already known fact that, when the combination of DESI BAO is done with different SN datasets, the evidence for evolving DE diminishes. For example, while the evidence is sizable using DES5Y or the Union3 datasets, milder evidence comes from using the Pantheon+ [7] SN dataset. It is of primary importance to understand whether the evidence is driven by one particular dataset, or if it supported by several of them. We will review thus the role of BAO itself and of SN datasets, to better understand how solid is the evidence coming from each of them.

The aim of our data analysis is actually two-fold. First, we will show that the DESI BAO data can be replaced by another recent measurement, namely the year-6 BAO measurement from the dark energy Survey (DES) [19], which consists of a single bin with 2.1% precision at $z = 0.85$. Combining this measurement with Planck and DES5Y SN we will compare to the fit that includes the DESI BAO data, with respect to the preference for evolving dark energy against ΛCDM.

Second, we will analyze the difference between SN datasets used in the analysis. In particular we look for evidence of evolving DE when combining together DES5Y with Pantheon+, by removing the common dataset. We will show, however, that this procedure is not unique, due to discrepancies in such a common dataset between the two catalogs. Indeed it has been recently pointed out [20] that in the DES5Y catalog the common SN have a rather different trend as a function of z, compared to the same SN in Pantheon+. In particular it has been claimed that such a common dataset in DES5Y has a $\sim$0.04 offset

JCAP04(2025)048

in magnitude between the low and high-redshift SN, which was not present in Pantheon+, and that once this offset is removed DES5Y leads to SN fits which are fully consistent with Pantheon+. For this reason we further explore the role of the common SN dataset in a more general analysis, leaving a free relative offset in magnitude between low and high redshift SN, and fitting to the full CMB+BAO+SN dataset.

The paper is organized as follows. In the next section we summarize the observables and the datasets used in the analysis. In section 3 we show the results by varying different BAO datasets. Later, in section 4 we fix the BAO from DESI and explore the impact of different SN catalogs, by carefully treating SN common to both DES5Y and Pantheon+ datasets. We summarize our findings in section 5. In appendix A we report the best fit parameters, mean and confidence intervals, based on the w_0w_aCDM parametrization determined through the Markov-Chain-Monte-Carlo for different datasets. Technical details of the SN datasets can be found in appendix B.

2 Observables and data

Our analysis depends on the cosmological model under consideration. As stated in the introductory section, we only consider two models: ΛCDM vs w_0w_aCDM. The latter refers to a DE component with equation of state phenomenologically parametrized in (1.2), which implies that its energy density evolves as,

$$\rho_{\rm DE} = \rho_c \Omega_{\rm DE} \exp(3w_a(a-1)) a^{-3(1+w_0+w_a)} \,. \tag{2.1}$$

Here $\rho_c \equiv 3M_{\rm Pl}^2 H_0^2$ is the critical density and we assume a spatially flat universe so that the energy densities ρ_i of DE, matter and radiation satisfy $\Omega_{\rm DE} + \Omega_m + \Omega_r = 1$, where $\Omega_i \equiv \rho_i/\rho_c$. Notice that for $w_0 = -1$ and $w_a = 0$ one recovers the cosmological constant.

CMB observables (meaning TT, TE, EE spectra and lensing) are important to the discussion because they constrain the input cosmological parameters, and they are always included in our analysis. Also, although the fluctuations of the w_0w_aCDM component have a limited impact on the CMB (see however [10] for more details), we always include them in our numerical computations following the prescription of [27] when the equation of state crosses the 'phantom' divide, i.e. $w < -1$. Note also that testing different Planck CMB likelihoods (e.g. PR3 and PR4) does not affect w_0, w_a constraints, as was shown in [1].

Of more direct connection with the focus of the paper are the observables of the BAO scales and SN luminosity fluxes.

BAO. The BAO ruler is the sound horizon at the epoch of baryon drag r_d, computed at redshift z_d and projected along the redshift, which is given by an integral

$$r_d \equiv \int_{z_d}^{\infty} dz' \frac{c_s(z')}{H(z')} \,, \tag{2.2}$$

where $c_s(z)$ is the sound speed of the photon-baryon fluid. The measurements of the BAO scale are reported as dimensionless ratios, i.e. the angular scale $D_M(z)/r_d$ for the transverse direction. Other measurements can be also performed along the line-of-sight using $D_H/r_d = 1/(H(z)r_d)$ or their isotropic combination $D_V/r_d \equiv (zD_H(z)D_M(z)^2)^{1/3}/r_d$, see [1].

JCAP04(2025)048

Category	Name	Description	Ref.
CMB	P18	Planck 2018 high-ℓ TT, TE, EE; low-ℓ TT; low-ℓ EE likelihoods; Planck 2018 lensing data.	[21]
SN	Pantheon+	Pantheon+ supernovae compilation.	[6, 7]
	DES5Y	DES5Y supernovae compilation. The likelihood has been derived by us using data and covariance found in [22], and it has been already used in [10] and cross-checked against the likelihood given in [23].	[8].
BAO	DESI_{BAO}	DESI 2024 BAO measurements. Redshift bins: $z = [0.3, 0.51, 0.71, 0.93, 1.32, 1.49, 2.33]$	[1]
	DES_{BAO}	DES BAO measurement at effective redshift $z = 0.85$	[19]
	BOSS_{BAO}	BAO measurements from 6dFGS at $z = 0.106$ [24], SDSS MGS at $z = 0.15$ [25] (BAO smallz), and CMASS and LOWZ galaxy samples of BOSS DR12 at $z = [0.38, 0.51, 0.61]$ [26]	[24–26]

Table 1. Datasets used in our work divided by categories (CMB, SN, BAO).

SN fluxes. Calibration of SN fluxes can be more subtle. The observed flux F of a Supernova with intrinsic luminosity L is a function of D_M, since $F \equiv L/(4\pi d_L^2)$, where the luminosity distance turns out to be $d_L = (1+z)D_M(z)$, i.e. the "distance duality" relation [28, 29]. It is common to report the magnitude:

$$\mu(z) \equiv 5\log_{10}[(1+z)D_M(z)] - M\,. \tag{2.3}$$

For our analysis here M is simply a nuisance parameter,[1] since it depends both on L and on the present-day Hubble rate H_0.[2] The SN datasets report the mean value and error of μ per each observation and their correlations via the covariance matrix.

2.1 Datasets used in this work

All the above observables are computed with the `CLASS` [32] Boltzmann solver. Our aim is to perform a Bayesian analysis to infer the posterior distributions of our cosmological parameters, and the Markov Chain Monte Carlo (MCMC) samples are generated through `MontePython` [33, 34]. The MCMC samples are then analyzed with `GetDist` [35] to produce all the posterior distributions and all the triangle plots of our paper.

In this work we consider three classes of datasets, corresponding to CMB, BAO and SN samples, as reported in table 1, to which we refer for the names used in the plots and the description of all individual datasets and likelihoods.

[1] We note that Pantheon+ and DES5Y catalogs have different conventions, and their M has a relative offset $\Delta M \approx 19.35$.

[2] Fixing this by the "distance ladder" method, as done by [30] would lead to a severe "Hubble tension" in both ΛCDM and w_0w_aCDM models. See instead [31] for a recent analysis with DESI data that can address the Hubble tension, by considering dark radiation models that modify r_d in the early Universe.

JCAP04(2025)048

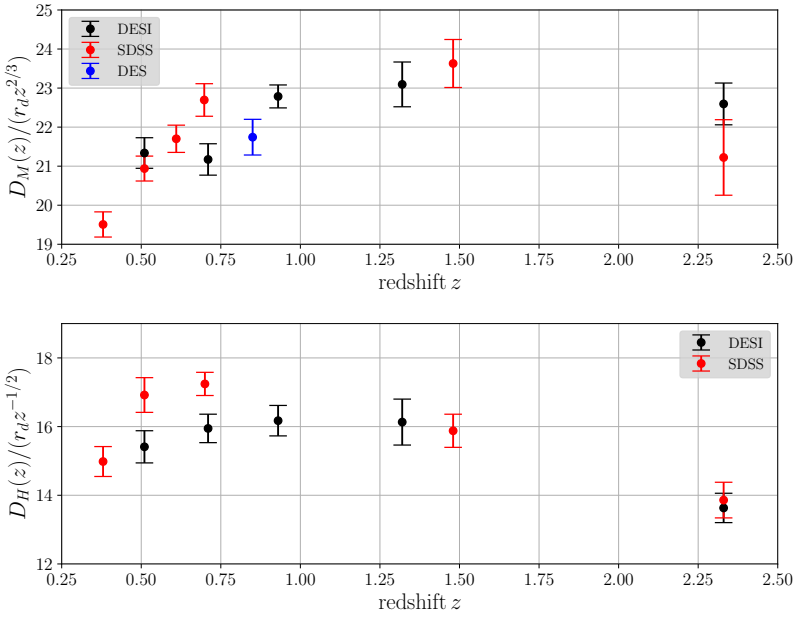

Figure 1. Part of the BAO dataset used in our work. For convenience we show $D_M(z)/(r_d z^{2/3})$ (upper panel) and $D_H(z)/(r_d z^{-1/2})$ (lower panel). Data for SDSS are taken from [36].

3 BAO likelihoods: DES vs DESI

In this section we are going to analyze the $w_0 w_a$CDM model with different combinations of datasets. In particular we are after the impact of the recent DESI and DES measurements of BAO scale. As discussed in the introduction, the recent DESI measurements of the BAO have attracted a lot of attention as they show a preference for evolving dark energy with equation of state $w \neq -1$. This happens when DESI is combined with CMB and DES5Y supernovae dataset. We refer the reader to [1] for all the details of the experimental analysis.

Here we combine a different BAO dataset to establish whether the evidence against ΛCDM found in [1] is confirmed at similar levels. The focus is to compare two different dataset combinations that only differ by the BAO set used, namely

$$\begin{aligned} &1) \quad \text{P18} + \text{DES5Y} + \text{BAO}_{\text{DESI}}\,, \\ &2) \quad \text{P18} + \text{DES5Y} + \text{BAO}_{\text{DES}}\,. \end{aligned} \tag{3.1}$$

whose likelihoods are listed in table 1. We also compare with previous BAO measurements from BOSS. For a visualization of part of the dataset see figure 1.

The measurement of the BAO scale in ref. [19] from the DES collaboration, that appeared before DESI, consists of a single very precise data point at $z = 0.85$ and it also shows a discrepancy with the ΛCDM best fit to the Planck data at 2.1σ. It is thus interesting to consider the impact of this result on the global fit when other measurements are also included. We thus perform a Bayesian analysis of evolving dark energy, replacing the DESI_{BAO} with the DES_{BAO} datapoint in the analysis of ref. [1].

We show in figure 2 and table 9 that DESY5 supernovae + DES_{BAO} (combined with Planck 2018 CMB TT+TE+EE spectra and Planck 2018 lensing data, P18 in short) has evidence

JCAP04(2025)048

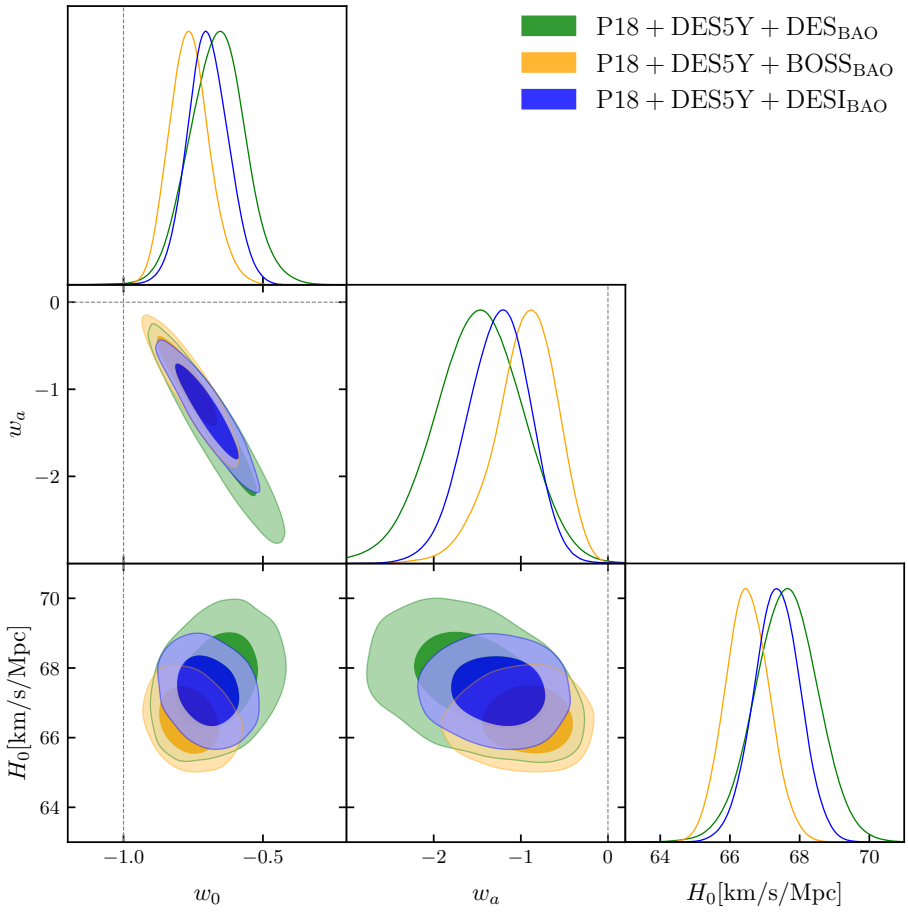

Figure 2. Marginalized posterior distributions for the parameters w_0, w_a and H_0 in the $w_a w_0$CDM model. All input parameters have uniform priors. The datasets included are P18 + DES5Y and BAO dataset (DES, in green; DESI, in blue; BOSS, in orange), as defined in table 1.

against ΛCDM. With such a dataset indeed the best-fit of $w_0 w_a$CDM has a $\Delta\chi^2 = -12$ compared to ΛCDM, leading to an exclusion of the latter model with a confidence level of 99.75%, i.e. 3σ, in the same direction of the 3.9σ exclusion obtained when using DESI as a BAO dataset. We have also performed a similar fit adding the DES$_{\rm BAO}$ bin to the DESI$_{\rm BAO}$ dataset, finding negligible differences with respect to the case where the BAO dataset is taken from DESI alone, which shows that there is good agreement between these two BAO datasets, providing a consistent picture (in contrast with previous BOSS data, which lead instead to quite different preferred regions: closer to ΛCDM and with lower H_0, see figure 2).

4 Supernovae likelihoods: DES5Y vs Pantheon+

In this section we critically review the role of supernovae in providing evidence for evolving DE. Our aim is to assess the role of different SN datasets, focusing on DES5Y and Pantheon+ and their possible combinations (see table 1 for all details).[3]

[3]A similar analysis was not possible for the Union3 dataset [9], which is not publicly available in unbinned form.

JCAP04(2025)048

Catalog	# tot.	$\#(z < 0.1)$	$\#(z > 0.1)$	# SNe	# tot. (com.)	# SNe (com.)
Pantheon+	1701	741	960	1543	375 (w/DES5Y)	335 (w/DES5Y)
DES5Y	1829	197	1632	1829	335 (w/Pantheon+)	335 (w/Pantheon+)
$\overline{\text{Pantheon+}}$	1326	511	815	1208	0 (w/DES5Y)	0 (w/DES5Y)
$\overline{\text{DES5Y}}$	1494	7	1487	1494	0 (w/Pantheon+)	0 (w/Pantheon+)

Table 2. Supernovae catalogs used (and constructed) in this work and their compositions. The sample $\overline{\text{Pantheon+}}$ and $\overline{\text{DES5Y}}$ are obtained by removing the SN in common with DES5Y and Pantheon+ respectively.

The DES5Y catalog has 1829 SN, including 335 supernovae in common with Pantheon+. The latter catalog has 1701 entries, but there are actually only 1543 supernovae (several SN appear more than once, since they actually are the same SN observed in different surveys). There are 375 entries in common with DES5Y (which correspond to 335 individual supernovae).

A preliminary summary of the composition of the two catalogs is provided in table 2. We also show the sample resulting in removing from DES5Y the supernovae in common with Pantheon+ (and viceversa). We call such samples, defined by having no supernovae in common between the two, $\overline{\text{DES5Y}}$ and $\overline{\text{Pantheon+}}$ respectively.

4.1 Combining the Pantheon+ and DES5Y supernovae datasets

Given the relevance of supernovae to establish the evidence for evolving dark energy it is tempting to try to include all the available data to increase the statistical significance. However it turns out that, due to a different treatment of the supernovae in common, such a combination is not univocal. Crucially this can be achieved in two ways: by removing the common dataset from DES5Y (obtaining the $\overline{\text{DES5Y}}$ dataset) or from Pantheon+ (obtaining the $\overline{\text{Pantheon+}}$ dataset), see table 2 for details. Once the common set is removed from one catalog we then combine with the other. While this procedure does not eliminate all the correlations between the datasets we believe that this first-stage analysis will be useful to determine the constraining power of the precise combination and the consistency of the two datasets.

In order to show the impact of these preliminary combinations we also combine Planck and DESI BAO datasets together with different SN samples. In particular we use the following combinations:

$$\begin{aligned} &1) \quad \text{P18} + \text{DESI} + \text{DES5Y}\,, \\ &2) \quad \text{P18} + \text{DESI} + \text{Pantheon+}\,, \\ &3) \quad \text{P18} + \text{DESI} + \overline{\text{DES5Y}} + \text{Pantheon+}\,, \\ &4) \quad \text{P18} + \text{DESI} + \overline{\text{Pantheon+}} + \text{DES5Y}\,. \end{aligned} \tag{4.1}$$

We perform the statistical analysis for ΛCDM and w_0w_aCDM in all four cases. The first two cases are again validated against the analysis of [1].

We find different results depending on which set of supernovae is discarded, shown in figure 3. The combination 3) where DESY5 common supernovae are discarded leads to results

JCAP04(2025)048

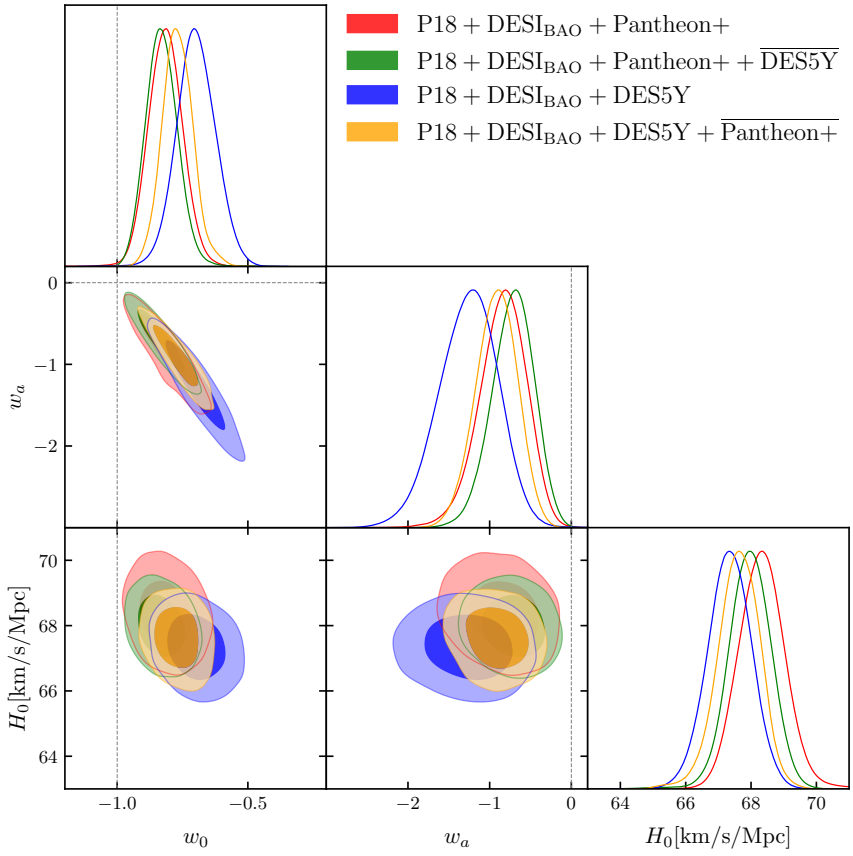

Figure 3. Marginalized posterior distributions for the parameters w_0, w_a and H_0 in the $w_a w_0$CDM model. All input parameters have uniform priors. The datasets included are P18 + DESI-BAO and a Supernovae sample. In particular we have tested four choices of SNe samples (DES5Y, blue; Pantheon+, red; Pantheon+ + $\overline{\rm DES5Y}$, green; DES5Y + $\overline{\rm Pantheon+}$, orange). Definitions are found in tables 1 and 2 and in section 4.1.

that are close to the case 2) where only the Pantheon+ catalog is included. This case is in milder disagreement with ΛCDM, i.e. disfavored at $\sim 2.5\sigma$. This is also consistent with the statement of ref. [20], as discussed in the next subsection, that the discrepancy with ΛCDM is mostly driven by the common subset in DES5Y. For the combination 4), where Pantheon+ common SNe are discarded we get instead a much stronger exclusion of ΛCDM, at about 3.8σ, similar to the case of DES5Y alone.

The fact that different combinations, that only differ for common SNe, lead to quantitatively different conclusions urges the need for a deeper understanding of the difference between Pantheon+ and DESY5 datasets to which we now turn.

4.2 Splitting the DES5Y supernovae dataset

The inspection of the common sample between DES5Y and Pantheon+ can have other implications. Indeed, recently, it has been pointed out in ref. [20] (see also [15] for related comments) that the supernovae in common between Pantheon+ and DES5Y appear, in the DES5Y catalog, with an offset between low ($0.025 < z < 0.1$) and high ($z > 0.1$) redshift

JCAP04(2025)048

magnitudes of about 0.04, due to different bias corrections applied in the DES5Y catalog. Let us comment on the fact that the composition of the DES5Y catalog strongly differs between low-z and high-z samples. Indeed, all the low-z external historical sample from previous surveys is in the first subset ($z < 0.1$), while the supernovae measured by the full five years of DES are mostly at $z > 0.1$ (with the exception of 3 supernovae). We refer to figure 5 for the composition of DES5Y as inferred from data in [22].

Ref. [20] argues that the larger preference against ΛCDM, compared to Pantheon+, in the analysis of [1] is due to such an offset. Our analysis will be more general, as we will show in the next subsections, but it is interesting to inspect the presence of the offset again simply by studying the magnitudes μ of the DES5Y sample (for the SNe in common with Pantheon+). As a preliminary step therefore we compare $\mu^{\rm DES/PAN}$ with the magnitudes computed in a flat ΛCDM reference model (with $\Omega_m = 0.306$), defining $\Delta\mu \equiv \mu - \mu_{\Lambda\rm CDM}$. We proceed to binning $\Delta\mu$ (see appendix) and we report the binned sample in the left panel of figure 4, where the offset is rather visible. Also, by applying a weighted average $\langle \ldots \rangle$ to the binned $\Delta\mu$ in the whole range of redshifts, we find that in the DES5Y sample in common with Pantheon+, $\langle \Delta\mu^{\rm DES} \rangle_{z<0.1} - \langle \Delta\mu^{\rm DES} \rangle_{z>0.1} = 0.045$. Here the weighted average is done with errors taken from the diagonal of the binned covariance matrix. Moreover, we note that in DES5Y all such common supernovae have smaller error bars than for Pantheon+, by an average overall factor of about 1.15.[4] This is most likely due to different light-curve fitting models and, in particular, to the use of different wavelength ranges.[5] In figure 4, we also observe that the correlation matrix (binned) reveals a significantly different pattern of correlations between the DES5Y and Pantheon datasets (in common). Notably, strong correlations are found among the very low-z sample in the DES5Y dataset, as seen in the center panel of figure 4. As shown in [20], the offset at low redshift receive a sizable contribution from SN belonging to the Foundation sample [40].

Finally, before going to the quantitative analysis, we wish to comment on the full DES5Y catalog displayed in figure 5. Also in the full sample, the nature of the low/high-z samples is rather different. We again proceed in defining $\Delta\mu$ and binning the full sample with the usual weights. From the correlation matrix of the full sample (see figure 5) we again see the strong correlation at low-z, and sizable correlation also in the very high-z bins, $z \gtrsim 0.5 - 0.6$, of the sample. This suggests to split the DES5Y catalog in two samples, also exploiting the not so large correlation between them.

A new split likelihood for DES5Y. Taking inspiration from the discussion so far, we consider the possibility of splitting the DES5Y dataset in two subsets. We introduce a relative offset δM between low and high z SN (we call the resulting modified dataset $\rm DES5Y_{split}$),

$$\rm DES5Y_{split} = DES5Y_{z<0.1, M+\delta M} \oplus DES5Y_{z>0.1, M} \,. \tag{4.2}$$

In practice, we have added a nuisance parameter δM to the magnitude of the low-z population.

[4] Such error bars are the ones that come from the diagonal of the covariance matrix in Pantheon+. Note however that this does not match with the error bars on the distance moduli provided by the collaboration [41], which are even larger, on average by another factor of 1.4.

[5] M.Vincenzi, private communication.

JCAP04(2025)048

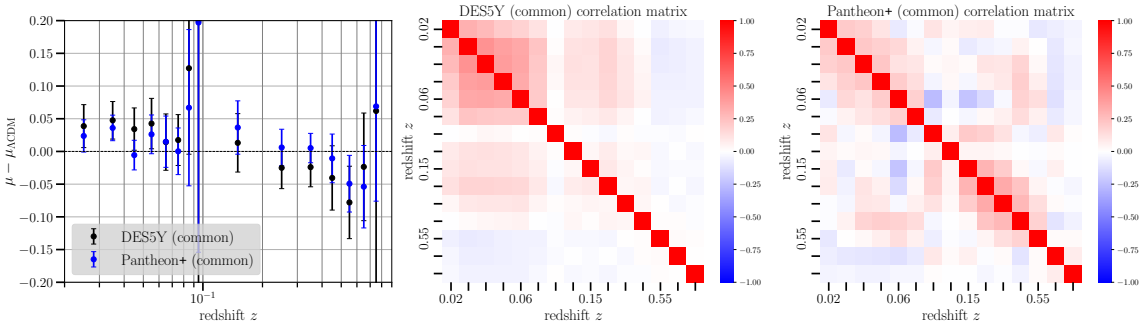

Figure 4. Pantheon+ and DES5Y common (binned) data samples. The weighted binning has been done as discussed in appendix B. In the left panel we show the weighted binning of SN magnitudes with respect to a ΛCDM reference model (see text) for both DES5Y and Pantheon+ for the SN in common between the two sample. In the center and right panels we show the binned correlation matrix of the corresponding samples.

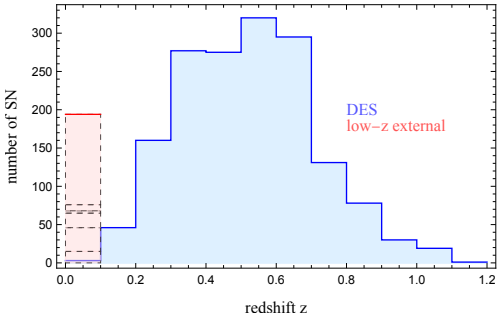

Surveys (ID)	#SN ($z < 0.1$)	#SN ($z > 0.1$)
DES [8]	3	1632
CFA3S [37]	15	0
CFA3K [37]	31	0
CFA4p2 [38]	19	0
CFA4p3 [38]	3	0
CSP [39]	8	0
FOUND [40]	118	0
total	197	1632

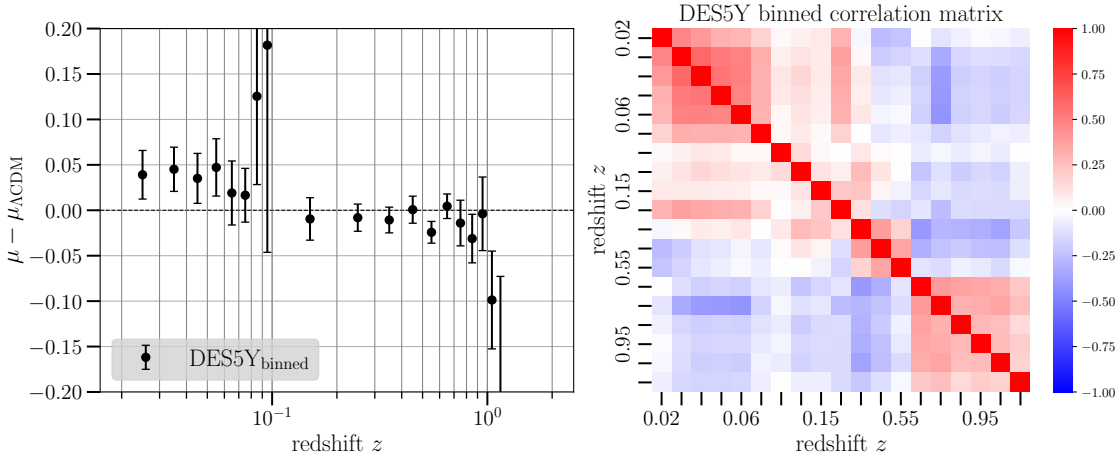

Figure 5. Composition of the full DES5Y sample. Upper Left: number of SN in different redshift bins of the DES5Y catalog. The low-z external data are shown in a stacked histogram. Upper Right: decomposition of DES5Y by surveys (at low and high redshift) as found on the dataset available from [22]. Lower left: weighted binning of SN magnitudes with respect to a ΛCDM reference model (see text). Lower right: Binned correlation matrix of the DES5Y sample.

JCAP04(2025)048

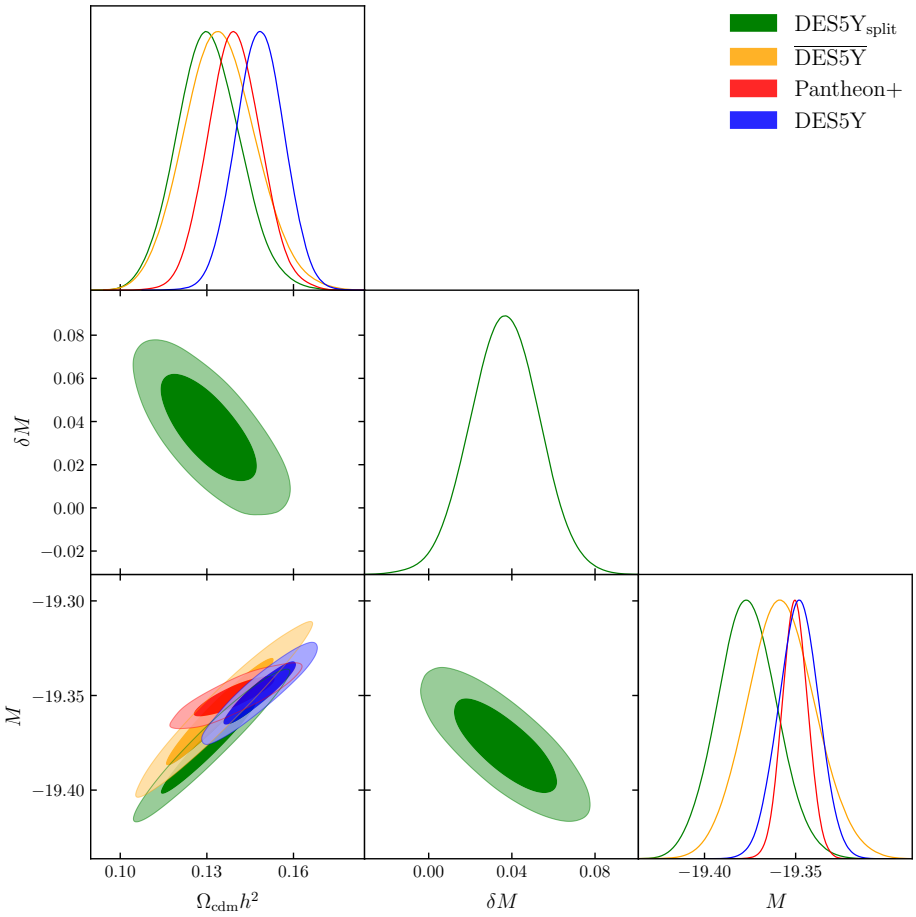

Figure 6. Marginalized posterior distributions for the parameters $\Omega_{\rm cdm}$, M and δM in ΛCDM model. All input parameters have uniform priors. We have only included in the fit the SNe datasets, corresponding to included are P18 + DESI-BAO and a Supernovae sample. We have tested four choices of SNe samples: DES5Y in blue, Pantheon+ in red, DES5Y$_{\rm split}$ in green, and $\overline{\rm DES5Y}$ in orange. Cf. tables 1 and 2 and sections 4.1 and 4.2. We have redefined the scale of M in $\overline{\rm DES5Y}$ by subtracting 19.37, in order to plot it together with Pantheon+.

Allowing δM to vary we first show in a simple ΛCDM fit with DES5Y$_{\rm split}$ alone that Ω_m gets smaller, and actually even smaller than the Pantheon+ value, see figure 6. Note also that a fit with $\overline{\rm DES5Y}$ alone yields a result for Ω_m in the same direction, which is consistent. This is because marginalizing over δM effectively ignores the overall low-z mean magnitude, a procedure similar to discarding the common sample, which contains almost all of the low-z data.

We then compare this new dataset with the usual DES5Y, fitting ΛCDM and w_0w_aCDM against the following full data combinations:

$$\begin{aligned} &1)\quad \text{P18} + \text{DESI} + \text{DES5Y}\,, \\ &2)\quad \text{P18} + \text{DESI} + \text{DES5Y}_{\rm split}\,, \end{aligned} \tag{4.3}$$

In figure 7 we show that indeed in the w_0w_aCDM model a nonzero shift is preferred, with $\delta M = 0.037 \pm 0.017$, and ΛCDM becomes now disfavored at 1.7 σ only.

JCAP04(2025)048

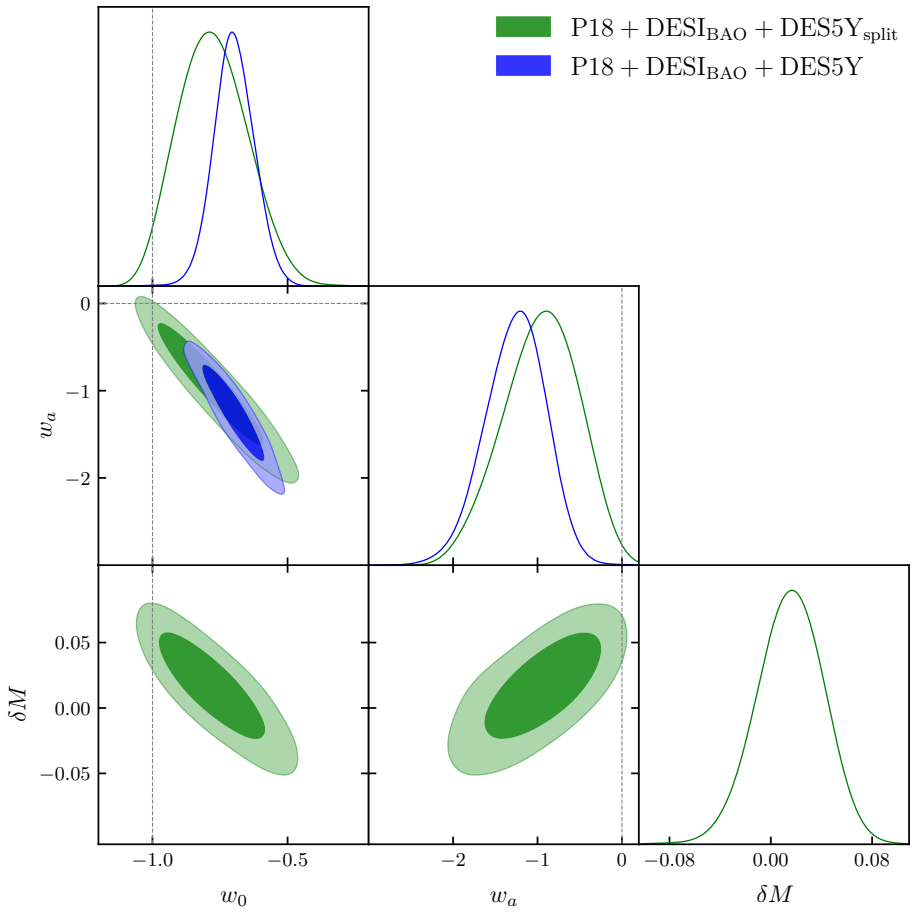

Figure 7. Marginalized posterior distributions for the parameters w_0, w_a and H_0 in the $w_a w_0$CDM model. All input parameters have uniform priors. The datasets included are P18 + DESI-BAO and a Supernovae sample. In particular we have tested the DES5Y$_{\rm split}$ sample (in green) compared to DES5Y (in blue). Their definitions can be found tables 1 and 2 as well as in section 4.2.

JCAP04(2025)048

5 Conclusions

At present, the sensitivity to time variations of dark energy relies on measurements of the BAO peak and spectrum as well as on (luminosity) distances inferred from supernovae observations. In this work, we re-examined the evidence disfavouring the ΛCDM model, showing the impact of slightly different treatments of the datasets. Our conclusions can be summarized in the following table:

Dataset	$\chi^2_{\rm min}(w_0w_a{\rm CDM})$	**ΛCDM** exclusion
P18+DESI$_{\rm BAO}$+DES5Y	4431	3.9σ
P18+DESI$_{\rm BAO}$+Pantheon+	4205	2.5σ
P18+DESI$_{\rm BAO}$+$\overline{\rm DES5Y}$ + Pantheon+	5550	2.5σ
P18+DESI$_{\rm BAO}$+$\overline{\rm Pantheon+}$ + DES5Y	5569	3.8σ
P18+DESI$_{\rm BAO}$+DES5Y$_{\rm split}$	4431	1.7σ
P18+DES$_{\rm BAO}$+DES5Y	4419	3σ

First, we have shown that the evidence in favour of a w_0w_aCDM parametrization of dark energy can be determined independently of the DESI$_{\rm BAO}$ sample. To support this we replaced the DESI$_{\rm BAO}$ data with the single BAO data point at $z = 0.85$ measured by DES (combined with DES5Y supernovae and P18 CMB data) finding a 3σ exclusion for ΛCDM. This result provides additional independent support for evolving dark energy.

Second, we have considered the possibility of combining different SN catalogs to increase the statistical significance. The combination is non-trivial due to the different treatment of the common SNe contained in Pantheon+ and DES5Y catalogues. In particular, for DES5Y we have shown that the treatment of such common supernovae is crucial: if we remove them from DESY5 and then combine with Pantheon+, we find overall agreement with results obtained using Pantheon+ alone, such that ΛCDM is only mildly disfavoured (at 2.5σ, in combination with P18+DESI$_{\rm BAO}$). If instead we perform the opposite combination, i.e. remove the common SNe from Pantheon+ and combining with the full DESY5 dataset, we find that ΛCDM is excluded at 3.8σ (in combination with P18+DESI$_{\rm BAO}$), similar to the fit without Pantheon+.

The different result of the SNe combination raises the question of the consistency of the catalogs. We have shown — compatibly with the observation of ref. [20] — that the disagreement can be accounted for by allowing different offsets in the DES5Y dataset for supernovae at redshifts $z > 0.1$ (where most of the new measurements are) and $z < 0.1$ (where all the old measurements are). Once this adjustment is made, the evidence against ΛCDM weakens to 1.7σ.

To conclude, while the BAO measurement by DES lends support to evolving dark energy, we believe that the consistency of the supernova sample from DES needs to be fully investigated in order to draw firm conclusion disfavouring ΛCDM based on combinations that include such a dataset.

JCAP04(2025)048

Acknowledgments

We wish to thank Elisabeta Lusso, Guido Risaliti and Marko Simonović for interesting discussions and Maria Vincenzi for feedback on the DES5Y dataset. We acknowledge the use of the computing resources provided by the "PC-Farm" at INFN Florence and by the "Nyx" cluster at ICCUB, Barcelona. A.N. is grateful to the Physics Department of the University of Florence for the hospitality during the course of this work. The work of AT and MR is supported by the Italian Ministry of University and Research (MUR) via the PRIN 2022 project n. 20228WHTYC. The work of A.N. is supported by the grants PID2019-108122GB-C32 from the Spanish Ministry of Science and Innovation, Unit of Excellence Maria de Maeztu 2020-2023 of ICCUB (CEX2019-000918-M) and AGAUR 2021 SGR 00872.

A Details of MCMC runs

Here we list the outcome of all our MCMCs for the w_0w_aCDM parametrization (w_0w_aCDM model), for all the data combinations, in tables 3–9. In all our chains we assume uniform priors on the input parameters. We also report the $\Delta\chi^2$ with respect to ΛCDM for the same dataset.

Parameter	Best-fit	Mean $\pm\sigma$	95% Lower	95% Upper
$100\ \omega_b$	2.234	$2.237^{+0.013}_{-0.014}$	2.209	2.264
$\omega_{\rm cdm}$	0.1202	$0.1198^{+0.0011}_{-0.00097}$	0.1178	0.1218
$100\theta_s$	1.042	$1.042^{+0.00029}_{-0.00029}$	1.041	1.042
$\ln(10^{10}A_s)$	3.052	$3.045^{+0.015}_{-0.015}$	3.016	3.076
n_s	0.966	$0.965^{+0.0036}_{-0.004}$	0.9575	0.9726
$\tau_{\rm reio}$	0.05776	$0.05494^{+0.0076}_{-0.0079}$	0.03956	0.07014
w_0	-0.7259	$-0.6948^{+0.073}_{-0.076}$	-0.8402	-0.5494
w_a	-1.249	$-1.275^{+0.4}_{-0.32}$	-1.981	-0.5855
$\Omega_{\rm DE}$	0.6862	$0.6835^{+0.0073}_{-0.0064}$	0.6702	0.6974
$M_{\rm DES}$	-0.04	$-0.04182^{+0.017}_{-0.017}$	-0.07421	-0.008567
H_0[km/s/Mpc]	67.73	$67.33^{+0.69}_{-0.64}$	66.03	68.67
σ_8	0.8158	$0.808^{+0.012}_{-0.01}$	0.7846	0.8304

$-\ln\mathcal{L}_{\rm min} = 2215.31$, minimum $\chi^2 = 4431$, $\Delta\chi^2 = -18$

Table 3. $\mathbf{w_0w_a}$CDM model with P18+DES5Y+$\rm DESI_{BAO}$ datasets.

JCAP04(2025)048

Parameter	Best-fit	Mean $\pm\sigma$	95% Lower	95% Upper
$100\,\omega_b$	2.237	$2.238^{+0.015}_{-0.016}$	2.208	2.268
$\omega_{\rm cdm}$	0.1197	$0.1199^{+0.0012}_{-0.0013}$	0.1175	0.1223
$100\theta_s$	1.042	$1.042^{+0.0003}_{-0.00029}$	1.041	1.042
$\ln(10^{10}A_s)$	3.046	$3.046^{+0.015}_{-0.015}$	3.016	3.076
n_s	0.9673	$0.9655^{+0.0043}_{-0.0043}$	0.9572	0.9739
$\tau_{\rm reio}$	0.05378	$0.05482^{+0.0073}_{-0.0079}$	0.03961	0.07025
w_0	-0.6401	$-0.6648^{+0.096}_{-0.096}$	-0.8529	-0.4745
w_a	-1.393	$-1.483^{+0.52}_{-0.47}$	-2.465	-0.4924
M	-0.03807	$-0.03245^{+0.03}_{-0.027}$	-0.0886	0.02331
H_0[km/s/Mpc]	67	$67.6^{+0.93}_{-0.91}$	65.81	69.42
σ_8	0.8104	$0.8098^{+0.015}_{-0.012}$	0.7822	0.8358

$-\ln\mathcal{L}_{\rm min} = 2209.71$, minimum $\chi^2 = 4419$, $\Delta\chi^2 = -12$

Table 4. $\mathbf{w_0w_a}$CDM model with P18+DES5Y+$\rm DES_{BAO}$ datasets.

Parameter	Best-fit	Mean $\pm\sigma$	95% Lower	95% Upper
$100\ \omega_b$	2.239	$2.232^{+0.014}_{-0.015}$	2.203	2.26
$\omega_{\rm cdm}$	0.1208	$0.1206^{+0.0011}_{-0.0011}$	0.1184	0.1228
$100\theta_s$	1.042	$1.042^{+0.0003}_{-0.0003}$	1.041	1.042
$\ln(10^{10}A_s)$	3.045	$3.047^{+0.015}_{-0.016}$	3.017	3.077
n_s	0.9617	$0.9632^{+0.004}_{-0.004}$	0.9552	0.971
$\tau_{\rm reio}$	0.05274	$0.05467^{+0.0074}_{-0.008}$	0.03939	0.07022
w_0	-0.8096	$-0.7687^{+0.071}_{-0.081}$	-0.9204	-0.6148
w_a	-0.609	$-0.948^{+0.45}_{-0.3}$	-1.763	-0.2027
$\Omega_{\rm DE}$	0.671	$0.6735^{+0.0079}_{-0.0069}$	0.6587	0.688
M	-0.08641	$-0.07236^{+0.016}_{-0.016}$	-0.1036	-0.04093
H_0[km/s/Mpc]	66.16	$66.53^{+0.62}_{-0.63}$	65.3	67.77
σ_8	0.8059	$0.7998^{+0.014}_{-0.011}$	0.7741	0.8239

$-\ln\mathcal{L}_{\rm min} = 2213.49$, minimum $\chi^2 = 4427$

Table 5. $\mathbf{w_0w_a}$CDM model with P18+DES5Y+$\rm BOSS_{BAO}$ datasets.

JCAP04(2025)048

Parameter	Best-fit	Mean $\pm\sigma$	95% Lower	95% Upper
$100\ \omega_b$	2.237	$2.238^{+0.014}_{-0.014}$	2.211	2.266
ω_{cdm}	0.12	$0.1196^{+0.00096}_{-0.0011}$	0.1178	0.1216
$100\theta_s$	1.042	$1.042^{+0.00029}_{-0.00028}$	1.041	1.042
$\ln(10^{10}A_s)$	3.028	$3.043^{+0.014}_{-0.015}$	3.016	3.073
n_s	0.964	$0.9656^{+0.004}_{-0.0036}$	0.9581	0.9729
$\tau_{\rm reio}$	0.04555	$0.05413^{+0.0065}_{-0.0075}$	–	–
w_0	-0.7994	$-0.8128^{+0.062}_{-0.067}$	-0.9378	-0.6849
w_a	-0.8319	$-0.8325^{+0.32}_{-0.24}$	-1.401	-0.2897
$\Omega_{\rm DE}$	0.6895	$0.694^{+0.0064}_{-0.0066}$	0.6817	0.7065
M	-19.4	$-19.39^{+0.019}_{-0.018}$	–	–
H_0[km/s/Mpc]	67.88	$68.3^{+0.68}_{-0.68}$	67	69.6
σ_8	0.8132	$0.8216^{+0.0095}_{-0.01}$	0.8016	0.8417

$-\ln\mathcal{L}_{\rm min} = 2102.41$, minimum $\chi^2 = 4205$, $\Delta\chi^2 = -8.7$

Table 6. $\mathbf{w_0w_a}$CDM model with P18+Pantheon+$+$DESI$_{\rm BAO}$datasets.

Parameter	Best-fit	Mean $\pm\sigma$	95% Lower	95% Upper
$100\ \omega_b$	2.24	$2.239^{+0.014}_{-0.014}$	2.212	2.266
ω_{cdm}	0.1194	$0.1195^{+0.001}_{-0.001}$	0.1175	0.1215
h	0.6783	$0.6798^{+0.0063}_{-0.0065}$	0.6676	0.6921
$\ln(10^{10}A_s)$	3.052	$3.045^{+0.014}_{-0.015}$	3.016	3.074
n_s	0.9658	$0.9658^{+0.0038}_{-0.004}$	0.9582	0.9733
$\tau_{\rm reio}$	0.05922	$0.05489^{+0.007}_{-0.0075}$	0.04006	0.06972
w_0	-0.8013	$-0.8308^{+0.059}_{-0.062}$	-0.9465	-0.7123
w_a	-0.7969	$-0.7134^{+0.28}_{-0.24}$	-1.226	-0.2132
$\Omega_{\rm DE}$	0.6903	$0.6914^{+0.0063}_{-0.0062}$	0.6792	0.7034
M	-19.4	$-19.4^{+0.018}_{-0.018}$	-19.44	-19.37
δM	0.004688	$-0.0008988^{+0.0088}_{-0.009}$	-0.01838	0.01663
H_0[km/s/Mpc]	67.83	$67.98^{+0.63}_{-0.65}$	66.76	69.21

$-\ln\mathcal{L}_{\rm min} = 2774.81$, minimum $\chi^2 = 5550$, $\Delta\chi^2 = -8.6$

Table 7. $\mathbf{w_0w_a}$CDM model with P18+Pantheon+$+\overline{\rm DES5Y}+$DESI$_{\rm BAO}$ datasets.

JCAP04(2025)048

Parameter	Best-fit	Mean $\pm\sigma$	95% Lower	95% Upper
$100\ \omega_b$	2.231	$2.239^{+0.013}_{-0.014}$	–	–
$\omega_{\rm cdm}$	0.12	$0.1196^{+0.00089}_{-0.00097}$	0.1177	0.1215
h	0.6745	$0.6765^{+0.0063}_{-0.0052}$	0.6654	0.6873
$\ln(10^{10}A_s)$	3.039	$3.043^{+0.013}_{-0.015}$	3.015	3.072
n_s	0.965	$0.9656^{+0.0037}_{-0.0035}$	0.9582	0.9726
$\tau_{\rm reio}$	0.05334	$0.05444^{+0.0071}_{-0.0076}$	–	–
w_0	−0.787	$-0.7727^{+0.059}_{-0.05}$	−0.8839	−0.6712
w_a	−0.8384	$-0.9048^{+0.27}_{-0.22}$	−1.404	−0.4223
$\Omega_{\rm DE}$	0.6857	$0.6882^{+0.0062}_{-0.0056}$	–	–
M	−19.42	$-19.41^{+0.016}_{-0.016}$	−19.44	−19.38
δM	0.0106	$0.00939^{+0.0075}_{-0.0069}$	−0.004954	0.02307
H_0[km/s/Mpc]	67.45	$67.65^{+0.63}_{-0.52}$	66.54	68.73

$-\ln\mathcal{L}_{\rm min} = 2784.73$, minimum $\chi^2 = 5569$, $\Delta\chi^2 = -17.4$

Table 8. $\mathbf{w_0w_a}$CDM model with P18+DES5Y+$\overline{\text{Pantheon+}}$+$\text{DESI}_{\text{BAO}}$datasets.

Parameter	Best-fit	Mean $\pm\sigma$	95% Lower	95% Upper
$100\ \omega_b$	2.238	$2.238^{+0.014}_{-0.014}$	2.21	2.266
$\omega_{\rm cdm}$	0.1201	$0.1197^{+0.0011}_{-0.001}$	0.1177	0.1217
h	0.682	$0.6798^{+0.01}_{-0.01}$	0.6594	0.6999
$\ln(10^{10}A_s)$	3.038	$3.043^{+0.014}_{-0.015}$	3.015	3.072
n_s	0.9634	$0.9653^{+0.0039}_{-0.0038}$	0.9579	0.973
$\tau_{\rm reio}$	0.05257	$0.05417^{+0.007}_{-0.0076}$	0.03976	0.0692
w_0	−0.8149	$-0.7753^{+0.11}_{-0.13}$	−0.9928	−0.5755
w_a	−0.8401	$-0.956^{+0.46}_{-0.37}$	−1.74	−0.2272
$\Omega_{\rm DE}$	0.6921	$0.6908^{+0.01}_{-0.0097}$	0.6711	0.7098
M	−0.04474	$-0.03981^{+0.016}_{-0.016}$	−0.07228	−0.007477
δM	0.02411	$0.01547^{+0.025}_{-0.023}$	−0.03109	0.06042
H_0[km/s/Mpc]	68.2	67.98^{+1}_{-1}	65.94	69.99

$-\ln\mathcal{L}_{\rm min} = 2215.59$, minimum $\chi^2 = 4431$, $\Delta\chi^2 = -4.9$

Table 9. $\mathbf{w_0w_a}$CDM model with P18+$\text{DES5Y}_{\text{split}}$+$\text{DESI}_{\text{BAO}}$ datasets.

JCAP04(2025)048

B Binned data samples

In each SN catalog we have access to the magnitude values μ_i and their covariance matrix σ_{ij} (including both statistical and systematical uncertainties), where the index runs over the full length of the catalog (see table 2). In all the numerical analysis of our paper we have worked with unbinned data samples, to exploit fully the correlations among different variables. However, in our discussion, we often refer to binned data sample for visualization purposes. We use a weighted binning procedure to define new magnitude variables $\hat{\mu}_\alpha$, where now the greek index α runs over the bins

$$\hat{\mu}_\alpha \equiv \frac{\sum_i w_{\alpha,i}\mu_i}{\sum_k w_{\alpha,k}} \equiv \sum_i B_{\alpha,i}\mu_i \,, \tag{B.1}$$

where the rectangular matrix B is such that $\sum_i B_{\alpha,i} = 1$ for all the rows (bins) α. Here $w_{\alpha,i}$ are generic weights that go to zero if the i-th variable μ_i does not belong to the α-th bin. Since our mapping is linear in the original variable, we can easily compute the covariance (and correlation) matrix $\hat{\sigma}_{\alpha\beta}$ of the new variables as

$$\hat{\sigma}_{\alpha\beta} = \frac{\sum_i w_{\alpha,i} \sum_j w_{\beta,j}\sigma_{ij}}{(\sum_k w_{\alpha,k})\,(\sum_l w_{\beta,l})} \,, \quad \mathrm{corr}_{\alpha\beta} \equiv \frac{\hat{\sigma}_{\alpha\beta}}{\sqrt{\hat{\sigma}_{\alpha\alpha}\hat{\sigma}_{\beta\beta}}} \,. \tag{B.2}$$

In figures 4 and 7 we adopted a weighted binning so defined: The edges of the bins are

$$\begin{aligned} z_{\text{bin edges}} = &[0.02\,, 0.03\,, 0.04\,, 0.05\,, 0.06\,, 0.07\,, 0.08\,, 0.09\,, 0.1\,, 0.2\,, 0.3\,, 0.4\,, 0.5\,, 0.6\,, \\ &0.7\,, 0.8\,, 0.9, 1\,, 1.1\,, 1.2]\,, \end{aligned} \tag{B.3}$$

and the center of each bin, defined as the average between two consecutive entries in the above list, z_α, is used to plot the corresponding quantities. The weights $w_{\alpha,i}$ are chosen to give more importance to the measurements μ_i with smaller errors, therefore we use the following expression

$$w_{\alpha,i} = \sigma_{ii}^{-1} \quad \forall i \in \mathrm{bin}_\alpha \,. \tag{B.4}$$

References

[1] DESI collaboration, *DESI 2024 VI: cosmological constraints from the measurements of baryon acoustic oscillations*, *JCAP* **02** (2025) 021 [arXiv:2404.03002] [INSPIRE].

[2] DESI collaboration, *DESI 2024: reconstructing dark energy using crossing statistics with DESI DR1 BAO data*, *JCAP* **10** (2024) 048 [arXiv:2405.04216] [INSPIRE].

[3] DESI collaboration, *DESI 2024: Constraints on physics-focused aspects of dark energy using DESI DR1 BAO data*, *Phys. Rev. D* **111** (2025) 023532 [arXiv:2405.13588] [INSPIRE].

[4] M. Chevallier and D. Polarski, *Accelerating universes with scaling dark matter*, *Int. J. Mod. Phys. D* **10** (2001) 213 [gr-qc/0009008] [INSPIRE].

[5] E.V. Linder, *Exploring the expansion history of the universe*, *Phys. Rev. Lett.* **90** (2003) 091301 [astro-ph/0208512] [INSPIRE].

[6] D. Scolnic et al., *The Pantheon+ Analysis: The Full Data Set and Light-curve Release*, *Astrophys. J.* **938** (2022) 113 [arXiv:2112.03863] [INSPIRE].

JCAP04(2025)048

[7] D. Brout et al., *The Pantheon+ Analysis: Cosmological Constraints*, *Astrophys. J.* **938** (2022) 110 [arXiv:2202.04077] [INSPIRE].

[8] DES collaboration, *The Dark Energy Survey: Cosmology Results with ∼1500 New High-redshift Type Ia Supernovae Using the Full 5 yr Data Set*, *Astrophys. J. Lett.* **973** (2024) L14 [arXiv:2401.02929] [INSPIRE].

[9] D. Rubin et al., *Union Through UNITY: Cosmology with 2,000 SNe Using a Unified Bayesian Framework*, arXiv:2311.12098 [INSPIRE].

[10] A. Notari, M. Redi and A. Tesi, *Consistent theories for the DESI dark energy fit*, *JCAP* **11** (2024) 025 [arXiv:2406.08459] [INSPIRE].

[11] O.F. Ramadan, J. Sakstein and D. Rubin, *DESI constraints on exponential quintessence*, *Phys. Rev. D* **110** (2024) L041303 [arXiv:2405.18747] [INSPIRE].

[12] S. Bhattacharya et al., *Cosmological constraints on curved quintessence*, *JCAP* **09** (2024) 073 [arXiv:2405.17396] [INSPIRE].

[13] D. Andriot et al., *Exponential quintessence: curved, steep and stringy?*, *JHEP* **08** (2024) 117 [arXiv:2405.09323] [INSPIRE].

[14] Y. Tada and T. Terada, *Quintessential interpretation of the evolving dark energy in light of DESI observations*, *Phys. Rev. D* **109** (2024) L121305 [arXiv:2404.05722] [INSPIRE].

[15] I.D. Gialamas et al., *Interpreting DESI 2024 BAO: Late-time dynamical dark energy or a local effect?*, *Phys. Rev. D* **111** (2025) 043540 [arXiv:2406.07533] [INSPIRE].

[16] W. Giarè et al., *Robust preference for Dynamical Dark Energy in DESI BAO and SN measurements*, *JCAP* **10** (2024) 035 [arXiv:2407.16689] [INSPIRE].

[17] W.J. Wolf, C. García-García, D.J. Bartlett and P.G. Ferreira, *Scant evidence for thawing quintessence*, *Phys. Rev. D* **110** (2024) 083528 [arXiv:2408.17318] [INSPIRE].

[18] J.-Q. Jiang, D. Pedrotti, S.S. da Costa and S. Vagnozzi, *Nonparametric late-time expansion history reconstruction and implications for the Hubble tension in light of recent DESI and type Ia supernovae data*, *Phys. Rev. D* **110** (2024) 123519 [arXiv:2408.02365] [INSPIRE].

[19] DES collaboration, *Dark Energy Survey: A 2.1% measurement of the angular baryonic acoustic oscillation scale at redshift zeff=0.85 from the final dataset*, *Phys. Rev. D* **110** (2024) 063515 [arXiv:2402.10696] [INSPIRE].

[20] G. Efstathiou, *Evolving Dark Energy or Supernovae Systematics?*, arXiv:2408.07175 [INSPIRE].

[21] PLANCK collaboration, *Planck 2018 results. V. CMB power spectra and likelihoods*, *Astron. Astrophys.* **641** (2020) A5 [arXiv:1907.12875] [INSPIRE].

[22] DES collaboration, *DES-SN 5YR Data Release*, https://github.com/des-science/DES-SN5YR,.

[23] Cobaya sampler, *DES5Y data*, https://github.com/CobayaSampler/sn_data/tree/master/DESY5.

[24] F. Beutler et al., *The 6dF Galaxy Survey: Baryon Acoustic Oscillations and the Local Hubble Constant*, *Mon. Not. Roy. Astron. Soc.* **416** (2011) 3017 [arXiv:1106.3366] [INSPIRE].

[25] A.J. Ross et al., *The clustering of the SDSS DR7 main Galaxy sample — I. A 4 per cent distance measure at z = 0.15*, *Mon. Not. Roy. Astron. Soc.* **449** (2015) 835 [arXiv:1409.3242] [INSPIRE].

[26] BOSS collaboration, *The clustering of galaxies in the completed SDSS-III Baryon Oscillation Spectroscopic Survey: cosmological analysis of the DR12 galaxy sample*, *Mon. Not. Roy. Astron. Soc.* **470** (2017) 2617 [arXiv:1607.03155] [INSPIRE].

JCAP04(2025)048

[27] W. Fang, W. Hu and A. Lewis, *Crossing the Phantom Divide with Parameterized Post-Friedmann Dark Energy*, *Phys. Rev. D* **78** (2008) 087303 [arXiv:0808.3125] [INSPIRE].

[28] B.A. Bassett and M. Kunz, *Cosmic distance-duality as a probe of exotic physics and acceleration*, *Phys. Rev. D* **69** (2004) 101305 [astro-ph/0312443] [INSPIRE].

[29] EUCLID collaboration, *Euclid: Forecast constraints on the cosmic distance duality relation with complementary external probes*, *Astron. Astrophys.* **644** (2020) A80 [arXiv:2007.16153] [INSPIRE].

[30] A.G. Riess et al., *A Comprehensive Measurement of the Local Value of the Hubble Constant with 1 km s^{-1} Mpc^{-1} Uncertainty from the Hubble Space Telescope and the SH0ES Team*, *Astrophys. J. Lett.* **934** (2022) L7 [arXiv:2112.04510] [INSPIRE].

[31] I.J. Allali, A. Notari and F. Rompineve, *Reduced Hubble tension in dark radiation models after DESI 2024*, *JCAP* **03** (2025) 023 [arXiv:2404.15220] [INSPIRE].

[32] D. Blas, J. Lesgourgues and T. Tram, *The Cosmic Linear Anisotropy Solving System (CLASS) II: Approximation schemes*, *JCAP* **07** (2011) 034 [arXiv:1104.2933] [INSPIRE].

[33] B. Audren, J. Lesgourgues, K. Benabed and S. Prunet, *Conservative Constraints on Early Cosmology: an illustration of the Monte Python cosmological parameter inference code*, *JCAP* **02** (2013) 001 [arXiv:1210.7183] [INSPIRE].

[34] T. Brinckmann and J. Lesgourgues, *MontePython 3: boosted MCMC sampler and other features*, *Phys. Dark Univ.* **24** (2019) 100260 [arXiv:1804.07261] [INSPIRE].

[35] A. Lewis, *GetDist: a Python package for analysing Monte Carlo samples*, arXiv:1910.13970 [INSPIRE].

[36] EBOSS collaboration, *Completed SDSS-IV extended Baryon Oscillation Spectroscopic Survey: Cosmological implications from two decades of spectroscopic surveys at the Apache Point Observatory*, *Phys. Rev. D* **103** (2021) 083533 [arXiv:2007.08991] [INSPIRE].

[37] M. Hicken et al., *CfA3: 185 Type Ia Supernova Light Curves from the CfA*, *Astrophys. J.* **700** (2009) 331 [arXiv:0901.4787] [INSPIRE].

[38] M. Hicken et al., *CfA4: Light Curves for 94 Type Ia Supernovae*, *Astrophys. J. Suppl.* **200** (2012) 12 [arXiv:1205.4493] [INSPIRE].

[39] K. Krisciunas et al., *The Carnegie Supernova Project I: Third Photometry Data Release of Low-Redshift Type Ia Supernovae and Other White Dwarf Explosions*, *Astron. J.* **154** (2017) 211 [arXiv:1709.05146] [INSPIRE].

[40] R.J. Foley et al., *The Foundation Supernova Survey: Motivation, Design, Implementation, and First Data Release*, *Mon. Not. Roy. Astron. Soc.* **475** (2018) 193 [arXiv:1711.02474] [INSPIRE].

[41] Pantheon+, *Pantheon+ dataset*, https://github.com/PantheonPlusSH0ES/DataRelease,.

JCAP04(2025)048